Biosensors and Bioelectronics 66 (2015) 392–398

Contents lists available at ScienceDirect

Biosensors and Bioelectronics

journal homepage: www.elsevier.com/locate/bios

Self-assembled dipeptide–gold nanoparticle hybrid spheres for highly sensitive amperometric hydrogen peroxide biosensors

Yufei Gong, Xu Chen*, Yanluo Lu, Wensheng Yang*

State Key Laboratory of Chemical Resource Engineering, Beijing University of Chemical Technology, Beijing 100029, PR China

ARTICLE INFO

Article history:
Received 8 August 2014
Received in revised form
6 November 2014
Accepted 17 November 2014
Available online 20 November 2014

Keywords:
Self-assembly of dipeptide
Gold nanoparticles
Hybrid sphere
Amperometric biosensor
H_2O_2

ABSTRACT

Novel self-assembled dipeptide–gold nanoparticle (DP–AuNP) hybrid microspheres with a hollow structure have been prepared in aqueous solution by a simple one-step method. Diphenylalanine (FF) dipeptide was used as a precursor to form simultaneously peptide spheres and a reducing agent to reduce gold ions to gold nanoparticles in water at 60 °C. Scanning electron microscopy (SEM) and transmission electron microscopy (TEM) revealed that formed AuNPs were localized both inside and on the surface of the dipeptide spheres. Horseradish peroxidase (HRP) as a model enzyme was further immobilized on the dipeptide–AuNP hybrid spheres to construct a mediate H_2O_2 amperometric biosensor. UV–vis spectroscopy showed that the immobilized HRP retained its original structure. Cyclic voltammetry characterization demonstrated that the HRP/dipeptide–AuNP hybrid spheres modified glassy carbon electrode showed high electrocatalytic activity to H_2O_2. The proposed biosensor exhibited a wide linear response in the range from 5.0×10^{-7} to 9.7×10^{-4} M with a high sensitivity of 28.3 μA mM^{-1}. A low detection limit of 1.0×10^{-7} M was estimated at $S/N=3$. In addition, the biosensor possessed satisfactory reproducibility and long-term stability. These results indicated that the dipeptide–AuNP hybrid sphere is a promising matrix for application in the fabrication of electrochemical biosensors due to its excellent biocompatibility and good charge-transfer ability.

1. Introduction

It is existed widely in nature and well-known that some biomolecules can self-assemble into various structures (Knowles et al., 2010). Molecular self-assembly is also a powerful, bottom-up approach for fabricating novel functional nano- or biomaterial (Whitesides and Grzybowski, 2002; Ulijn and Smith, 2008). Recently, a peptide-based self-assembly is attracting increasing attention due to inherent biocompatibility, chemical versatility, biological recognition, and facile synthesis (Gazit, 2007; Hamley, 2014). Among various peptide-based building blocks, diphenylalanine (Phe – Phe, FF) and its derivatives are simplest ones that can form various nanostructures exhibiting novel optical, mechanical and electrochemical properties (Panda et al., 2008; Ryu et al., 2009; Yemini et al., 2005b). These fascinating properties make them potential as a kind of attractive and versatile materials for biosensor applications. Gazit and coworkers firstly reported that FF self-assembled peptide nanotubes (PNTs) as a novel electrochemical biosensing platform showed promising analytical performance (Yemini et al., 2005a). Thereafter PNTs were applied in the encapsulation of various biomolecules for electrochemical biosensing (Adler-Abramovich et al., 2010; Park et al., 2012; Sasso et al., 2012; Castillo et al., 2013; Baker et al., 2014). Furthermore, semiconductor quantum dots (such as CdTe and CdSe) and enzymes have been together introduced into the self-assembly of N-fluorenylmethoxycarbonyl diphenylalanine (Fmoc-FF) (Kim et al., 2011b). The optical biosensors based on the self-assembled quantum dot-peptide hydrogel composite have been successfully developed. Despite these advances, the further tuning FF-based peptide nanostructures and the introduction of more functional units into peptide entities are still highly desirable for the design of novel biosensor and the improvement of the sensing performance (de La Rica et al., 2011; Qu et al., 2014).

Noble metal nanoparticles such as gold nanoparticles (AuNPs) have been extensively employed for the preparation of inorganic–organic hybrid materials and applied in electrochemical biosensors (Zhang et al., 2010; Wang et al., 2012). Due to their excellent conductivity, good biocompatibility and high surface area, the analytical performances of the biosensors based on AuNPs hybrid systems could be significantly enhanced relative to those based on only organic components. Compared with general organic compounds, the biological molecules, especially for peptides, have unique advantages in preparing well-designed AuNP hybrid

* Corresponding authors. Fax: +86 10 64425385.
E-mail addresses: chenxu@mail.buct.edu.cn (X. Chen), chenxu@mail.buct.edu.cn (W. Yang).

http://dx.doi.org/10.1016/j.bios.2014.11.029
0956-5663/

nanostructures because of their abundant constitutes, specific chelate ability to inorganic ions and easy control of the crystal structure (Dickerson et al., 2008; Chen and Rosi, 2010; Song et al., 2010). However, the studies on the combination of AuNPs and FF self-assembled nanostructures are very limited (Yan et al., 2010a). To the best of our knowledge, no other group has reported the functionalization of dipeptide spheres with AuNPs for the immobilization of enzyme to construct electrochemical biosensor.

Herein, considering the above mentioned advantages of self-assembled dipeptide nanostructures and AuNPs, novel dipeptide–AuNP hybrid spheres with hollow structure were synthesized through a simple self-assembly process. Such composites were further employed to immobilizing a model enzyme, horseradish peroxidase (HRP), for the construction of an electrochemical H_2O_2 biosensor. Hydroquinone (HQ) was chosen as an electron-mediator (Camacho et al., 2009; Won et al., 2010). Electrochemical measurements were conducted to investigate the catalytic performance of the proposed biosensor. The good properties of the biosensor based on the dipeptide–AuNP hybrid spheres were demonstrated.

2. Experimental section

2.1. Materials

Diphenylalanine (FF) peptide in a lyophilized form was obtained from Bachem (Bubendorf, Switzerland). 1,1,1,3,3,3-Hexafluoro-2-propanol (HFIP) was purchased from Aladdin Chemicals Co. Ltd., China. The $HAuCl_4 \cdot 4H_2O$ (99.9%) was purchased from Sinopharm Chemical Reagent Co. Ltd., China. Horseradish peroxidase (HRP, RZ ≥ 3, activity ≥ 250 units mg^{-1}) was obtained from Shanghai Xueman Biotechnology Co. Ltd. (China). Hydroquinone (HQ) was purchased from Tianjin Fuchen Chemical Reagent Works (China). Hydrogen peroxide (H_2O_2, 30%) was obtained from Beijing Chemical Works (China). Nafion (5 wt%) was purchased from Sigma-Aldrich. The solutions used for electrochemical characterization were freshly prepared using 0.1 M of phosphate buffer solution (PBS, pH 7.0) unless otherwise noted. All other reagents were of analytical grade and used without further purification. All solutions were prepared with deionized, doubly distilled water (DDW).

2.2. Preparation of dipeptide–AuNP Hybrid spheres

A FF stock solution was freshly prepared by dissolving the lyophilized FF in HFIP at a concentration of 100 mg mL^{-1}. The stock solution was then diluted with 0.5 mM $HAuCl_4$ solution to a final concentration of 2 mg mL^{-1}. The mixture solution was stirred for 30 min, followed by incubation at 60 °C in the dark for 1.5 h. The color of the solution changed from light yellow to light purple. The suspension of the dipeptide–AuNP hybrid spheres was prepared. Herein, the synthesized conditions have been optimized to obtain the hybrid spheres with good morphology and uniform structure according to the concentration of peptide and $HAuCl_4$, as well as synthesized temperature and time.

2.3. Preparation of HRP/dipeptide–AuNP hybrid sphere modified electrodes

Prior to use, glassy carbon electrodes (GCE, diameter 3 mm) were first polished with 1.0, 0.3, and 0.05 μm alumina slurry sequentially, followed by rinsing with DDW, sonicating and then drying by nitrogen. Enzyme electrode was fabricated by a simple casting method. An aliquot (6 μL) of the dipeptide–AuNP hybrid sphere suspension was dropped on the pretreated GCE and left to dry at room temperature. Then 2 mg mL^{-1} of HRP solution (6 μL) was dropped on the dipeptide–AuNP hybrid sphere modified GCE and dried at 4 °C overnight in a humidity chamber. The electrode was then coated with 3 μL of 0.5 wt% Nafion solution and dried at 4 °C. Finally the modified electrode was washed gently with DDW three times to remove unbounded enzyme, denoted as a HRP/DP–AuNP/GCE. In control experiment, a HRP/GCE without dipeptide–AuNP hybrid spheres was also fabricated using the same procedure. The as-prepared electrodes were stored at 4 °C when not in use.

2.4. Instruments and measurements

Scanning electron microscopy (SEM) images were recorded with a Zeiss Supra 55 field emission scanning electron microscope equipped with energy-dispersive X-ray spectroscopy (EDS). Transmission electron microscopy (TEM) images were obtained on a Hitachi H-800 electron microscope with an accelerating voltage of 200 kV. For the SEM and TEM measurements, the suspension of the dipeptide–AuNP hybrid sphere was dropped onto a silicon wafer and a copper grid, respectively, followed by drying at room temperature. UV–vis absorbance spectra were recorded on a UV–vis spectrophotometer (Perkin-Elmer Lambda 35).

Electrochemical experiments were conducted on a CHI 660B electrochemical workstation (Shanghai CH Instruments, China). A conventional three-electrode system was employed with a modified glassy carbon electrode as the working electrode, a platinum wire as the counter electrode, and a saturated Ag/AgCl electrode as the reference electrode. The cyclic voltammetric measurements were carried out in an unstirred electrochemical cell. Amperometric curves were obtained by consequently adding H_2O_2 solution with a certain concentration into PBS containing 1.0 mM HQ at -0.05 V after achieving a steady state current. The working solutions were deoxygenated with nitrogen gas for 15 min before measurements and a nitrogen atmosphere was kept over the solutions throughout the experiments.

3. Results and discussion

3.1. Morphological characterization and formation mechanism of the dipeptide–AuNP hybrid spheres

The strategy employed to prepare the dipeptide–AuNP hybrid spheres and the HRP-based biosensor was illustrated in Scheme 1. Firstly, the FF/HFIP monomer solution was added into the $HAuCl_4$ solution. After 60 °C for 1.5 h, the color of the solution changed from light yellow to light purple, indicating that the gold ions were reduced to form AuNPs (Tan et al., 2010; Kim et al., 2011a). The obtained solution was characterized in detail by SEM and TEM, as shown in Fig. 1. The sub-micrometer peptide spheres with embedded AuNPs were observed from the SEM image (Fig. 1A). The average diameter of the hybrid spheres and AuNPs was about 812 nm and 27 nm, respectively. EDS analysis (Fig. 1B) confirmed that the elemental composition of the hybrid spheres. TEM images (Fig. 1C and D) further showed that the AuNPs were not only localized on the surface of the dipeptide spheres, but also embedded inside the hybrid spheres (see Fig. S1). Furthermore, the partially aggregated AuNPs and the hollow structure in the hybrid spheres were also observed from TEM images. For the fabrication of the modified electrode, the obtained dipeptide–AuNP hybrid spheres were further casted onto the GCE surface, and then the HRP solution was also casted onto the surface of the hybrid sphere modified GCE. Finally, they were enclosed to the electrode surface by coating Nafion membrane as protective additive, which is widely used in the preparation of electrochemical biosensors (Wang et al., 2010; Park et al., 2012; Baker et al., 2014).

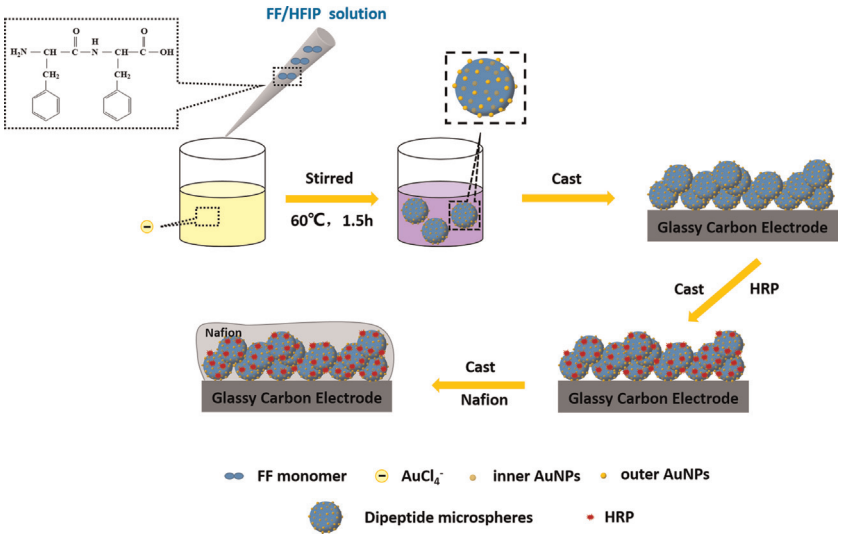

Scheme 1. Schematic illustration of the synthesis of dipeptide–AuNP hybrid spheres and the fabrication of the HRP/DP–AuNP modified GCE. (For interpretation of the references to color in this figure legend, the reader is referred to the web version of this article.)

The formation mechanism of the dipeptide–AuNP hybrid spheres was preliminarily investigated. Incubation of $HAuCl_4$ in the absence of dipeptide at 60 °C for 1.5 h did not result in the formation of any precipitates or color change of the solution (data not shown), indicating that the FF dipeptide acted as a reductant of gold ions. It has been demonstrated in the previous study (Nayak and Shin, 2006) that L-phenylalanine (F) can reduce gold salts to form zero valent gold nanoparticles without adding any reducing agent under boiling conditions. Herein, the amino group in the dipeptide might play a role as mild reducing element. Moreover, the self-assembly of alone FF monomer solution at the same synthesized condition only in the absence of $HAuCl_4$ did not lead to the formation of spherical structure, but rather tubal structures (see Fig. S2). This suggested that the presence of gold ions in the self-assembled FF solution not only played a role in introducing gold nanoparticles and resulting in the functional peptide composites, but also affecting the self-assembly of dipeptide and finally changing the morphology of peptide nanostructures. According to previously reported the self-assembly mechanism of the FF dipeptide (Reches and Gazit, 2004 and 2006) and the other peptide–AuNP hybrids (Song et al., 2010; Kim et al., 2011a), a possible formation mechanism of the dipeptide–AuNP hybrid spheres obtained in the present work was proposed and showed in Fig. S3.

Firstly, when the FF monomers were added into the solution of gold ions, $AuCl_4^-$ ions were adsorbed on protonated amine groups of the dipeptide due to electrostatic interaction (Nayak and Shin, 2006). And then FF monomers along with adsorbed $AuCl_4^-$ could self-assemble rapidly into a two-dimensional (2D) sheet layer due to a π–π stacking interaction between aromatic moieties of the dipeptides (Reches and Gazit, 2004; Gazit, 2007). When the solution temperature increased to 60 °C, the reduction of gold ions to AuNPs by the dipeptide happened. With increasing the reaction time, the AuNPs began the nucleation and further growth. Simultaneously, the extended 2D sheet layer could be closured by along two axes, finally leading to the formation of the hybrid spheres (Reches and Gazit, 2006; Yan et al., 2010b). Herein, the FF dipeptides acted as both reducing agent and linking molecule to provide the certain morphology. Overall, the synergistic action of gold ion and FF dipeptide at the suitable temperature, i.e. the simultaneous self-assembly of peptides and nucleation of gold ion via the interaction of both reactants, finally resulted in the formation of the novel dipeptide–AuNP hybrid spheres. Due to combining the advantages of dipeptides and AuNPs, the hybrid sphere was further used as an immobilized matrix of HRP and applied in the electrochemical biosensor for H_2O_2.

3.2. UV–vis spectroscopic characterization of the HRP/dipeptide–AuNP hybrid spheres

The Soret band of protein UV–vis spectrometry is sensitive to the variation of the micro-environment around the heme group and can provide information about the conformational integrity of the proteins (Singh et al., 2013). Fig. 2 shows the UV–vis absorption spectra of different samples. The dipeptide–AuNP hybrid spheres showed a weak absorption peak at 570 nm (Fig. 2a), which is characteristic of AuNPs. This peak could be also observed in the HRP/dipeptide–AuNP hybrid spheres. Moreover, the Soret absorptions of the HRP entrapped on the dipeptide–AuNP hybrid spheres (Fig. 2b) and the native HRP (Fig. 2c) were located at nearly the same wavelength (about 402 nm), suggesting that dipeptide–AuNP hybrid spheres had good biocompatibility and the original structure of the immobilized HRP did not changed.

3.3. Electrochemical response of the HRP/DP–AuNP/GCE to H_2O_2

In order to construct a H_2O_2 biosensor, the HRP/DP–AuNP/GCE was fabricated as a working electrode. HQ was used as an excellent electron mediator of shuttling electrons between the redox center of the HRP and the surface of the GCE. Fig. 3 shows the cyclic voltammograms (CVs) of the HRP/DP–AuNP/GCE (A) and the HRP/GCE (B) before and after the addition of H_2O_2 in 0.1 M PBS solution containing 1.0 mM HQ. In the absence of H_2O_2, a pair of redox peak was observed at the two enzyme electrodes (curve a in Fig. 3), which is characteristic of redox process of HQ. With increasing scan rates from 20 to 320 mV s^{-1}, both the anodic and cathodic peak currents of the HRP/DP-AuNP/GCE increased, and also the peak currents were proportional to the square root of the scan rate (Fig. S4). Similar to the previous reports (Silvestrini et al., 2013; Martin et al., 2014), this indicated a diffusion-controlled process.

When 2 mM H_2O_2 was added into the solution, the cathodic peak current of the HRP/DP–AuNP/GCE increased significantly,

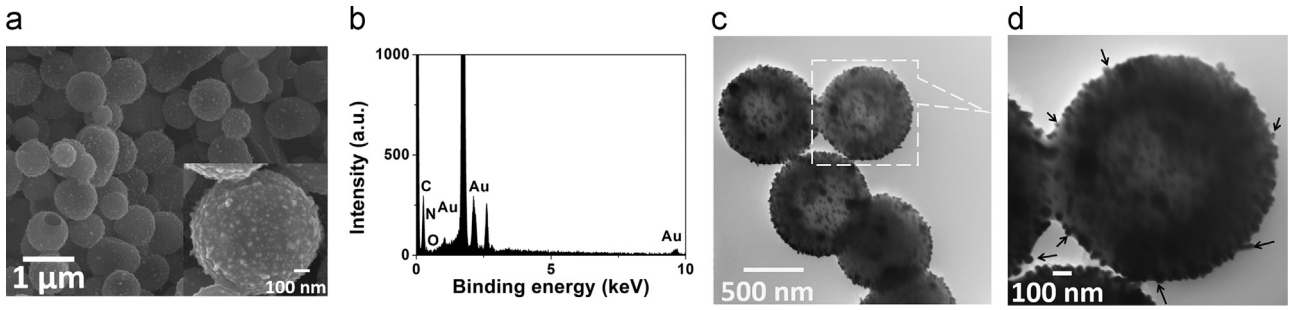

Fig. 1. (A) SEM images, (B) EDS analysis and (C, D) TEM images of dipeptide–AuNP hybrid spheres. The inset in (A) is the high magnification view. The black arrow in (D) marked embedded AuNPs.

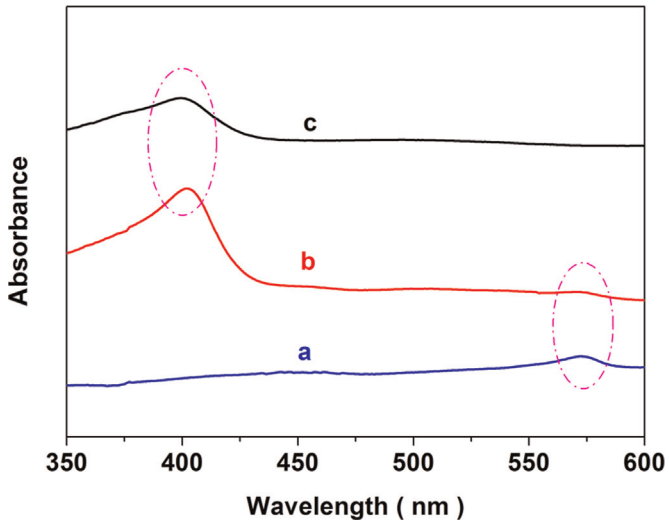

Fig. 2. UV–vis absorption spectra of various films on the quartz slide. (a) dipeptide–AuNP hybrid spheres, (b) HRP/dipeptide–AuNP hybrid spheres and (c) HRP film.

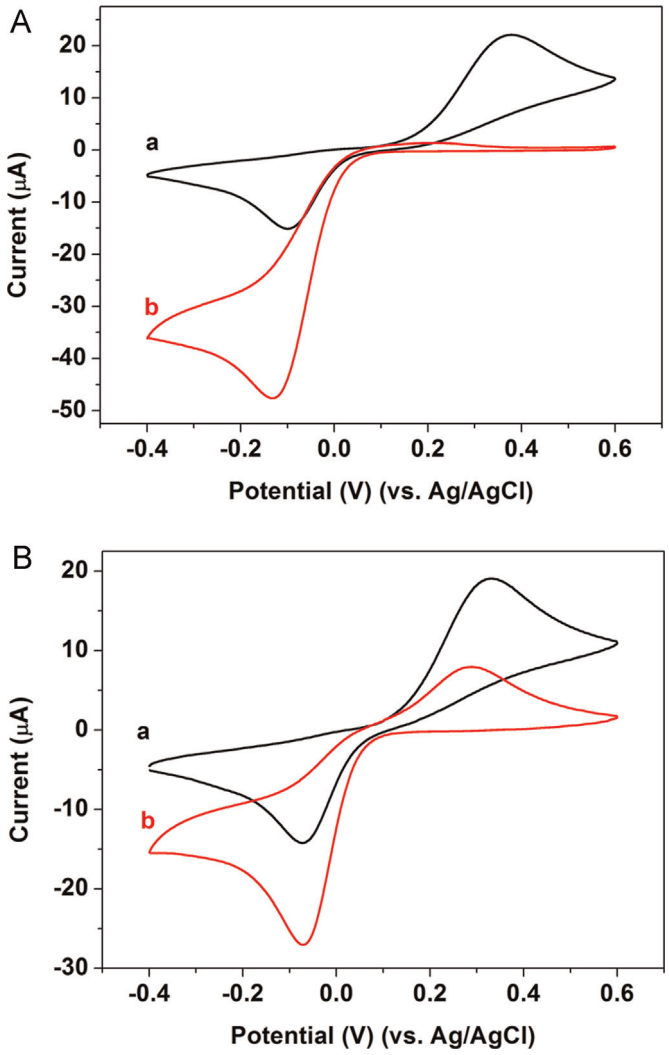

Fig. 3. CVs of 1.0 mM HQ in N_2-saturated 0.1 M PBS (pH 7.0) at the HRP/DP–AuNP/GCE (A) and the HRP/GCE (B) in the absence (a) and presence (b) of 2.0 mM H_2O_2. Scan rate, 100 mV s^{-1}.

accompanied by a decrease of the anodic peak current (curve b in Fig. 3A). This is a typical electrocatalytic effect of HRP to the reduction of H_2O_2. The reaction mechanism of the HQ-mediator HRP biosensor has been reported as follows (Wang et al., 2012):

$$HRP_{(red)} + H_2O_2 \rightarrow HRP_{(ox)} + H_2O \quad (1)$$

$$HRP_{(ox)} + HQ_{(red)} \rightarrow HRP_{(red)} + HQ_{(ox)} \quad (2)$$

$$HQ_{(ox)} + 2H^+ + 2e^- \rightarrow HQ_{(red)} \quad (3)$$

When H_2O_2 was added into the solution, H_2O_2 was firstly reduced by the immobilized $HRP_{(red)}$. Then the HRP could be regenerated with the aid of HQ, while the mediator $HQ_{(red)}$ could be oxidized to $HQ_{(ox)}$. Finally, the produced $HQ_{(ox)}$ was electrochemically reduced on the HRP/DP–AuNP/GCE, leading to a great increase of the reduction current. Furthermore, the CVs of the DP–AuNP/GCE (no HRP) exhibited no notable difference in the absence and presence of H_2O_2 (Fig. S5), indicating that the catalytic effect was mainly attributed to the immobilized HRP. In addition, the electrocatalytic peak current obtained on the HRP/GCE (curve b in Fig. 3B) was much lower than that on the HRP/DP–AuNP/GCE (curve b in Fig. 3A) in the presence of the same concentration of H_2O_2. This suggested that the HRP immobilized on the dipeptide–AuNP hybrid spheres presented better electrocatalytic activity toward H_2O_2. It might be attributed to the combined effects of the biocompatible peptide and AuNPs with high conductivity. Based on the principle that the increased reduction current value of the HRP/DP–AuNP/GCE was proportional to the concentration of added H_2O_2, the H_2O_2 analyst could be further detected on the biosensor.

3.4. Optimization of experimental parameters

In order to obtain the maximum sensitivity of the biosensor, the experimental parameters were optimized through current responses for 0.5 mM H_2O_2 at the HRP/DP–AuNP/GCE (Fig. S6). The effect of the immobilized amount of HRP on the response of the

biosensor was firstly examined (Fig. S6A). The current response of the modified electrode increased sharply with increasing the amount of HRP to the maximal value of 6 μL, and then tended to steady, even unconspicuous decreased with further increases in the amount of HRP. This may be ascribed to larger amount of HRP beyond 6 μL could not be effectively absorbed, and even hindered the electron transfer due to its non-conducting state. Then 6 μL of the HRP was used for the further experiment.

Furthermore, the influence of the solution pH on the response of the HRP/DP–AuNP/GCE was also checked in the 6.0–8.0 pH range (Fig. S6B). The current exhibited an almost bell-shaped behavior with the highest response at pH 7.0. The value of solution pH could influence the enzyme activity of HRP and electrochemical behavior of the HQ mediator including the reduction peak current and peak potential. The high response of the biosensor at neutral solution was probably attributed to two aspects. On one hand, the optimum enzyme activity for soluble HRP was reported at pH 7.0 (Wang and Zhang, 2006) and the good biocompatibility of the dipeptide–AuNP hybrid sphere maintained the high enzyme activity of HRP at same pH. On the other hand, the highest peak current of HQ was often obtained in near neutral solution (Yin et al., 2011; Han et al., 2014) and its reduction peak potential was close to the applied potential of −0.05 V. Therefore the following experiments were performed at pH 7.0.

The optimum concentration of mediator HQ was determined (Fig. S6C). It was found that the current increased with the concentration of HQ and reached a plateau at 1.0 mM. Such behavior is typical of a mediator-based sensor (Xiao et al., 1999). At a low HQ concentration the current response was limited by enzyme-mediator kinetics. On the other hand, when the HQ concentration was too high, it resulted in a response limited by enzyme–substrate kinetics. Moreover, a higher concentration of mediator might produce a larger background current. Hence, 1.0 mM HQ was selected for further studies.

In addition, the effect of the applied potential on the response of the biosensor was further evaluated in the potential range from 0 V to −0.2 V (Fig. S6D). The current increased remarkably when the applied potential shifted from 0 V to −0.05 V and then increased slowly for potentials beyond −0.05 V. The current increase was attributed to the increased driving force for the fast reduction of HQ at low potential (Chen et al., 2001). Although the sensor could have a higher response at −0.20 V, a working potential of −0.05 V was chosen for the following amperometric determination of H_2O_2. At this potential, relatively sufficient current response was obtained, at the same time the background current was minimized and the possible interference from other electroactive species could be avoided or reduced.

3.5. Amperometric performance of the biosensor

Under the optimum conditions, the performance of the constructed biosensor was investigated by the amperometric method. Fig. 4A shows typical current–time curves for the HRP/DP–AuNP/GCE (a) and the HRP/GCE (b) with successive injections of H_2O_2. When the analyte was added to the stirred PBS, the reduction currents increased rapidly and 95% of the steady-state current was obtained within 8 s. The corresponding calibration curves for H_2O_2 were given in Fig. 4B. The HRP/DP–AuNP/GCE (curve a in Fig. 4B) showed a wide linear range from 5.0×10^{-7} to 9.7×10^{-4} M with a correlation coefficient of 0.998. The biosensor also exhibited a high sensitivity of 28.3 μA mM^{-1}. A detection limit was estimated to be 1.0×10^{-7} M at a signal to noise ratio of 3. Meanwhile the control HRP/GCE (curve b in Fig. 4B) showed the lower sensitivity (10.8 μA mM^{-1}) and higher detection limit (4.3×10^{-6} M) compared with the HRP/DP–AuNP/GCE.

The comparison of the analytical performances of recently reported H_2O_2 biosensors based on the AuNPs composites was

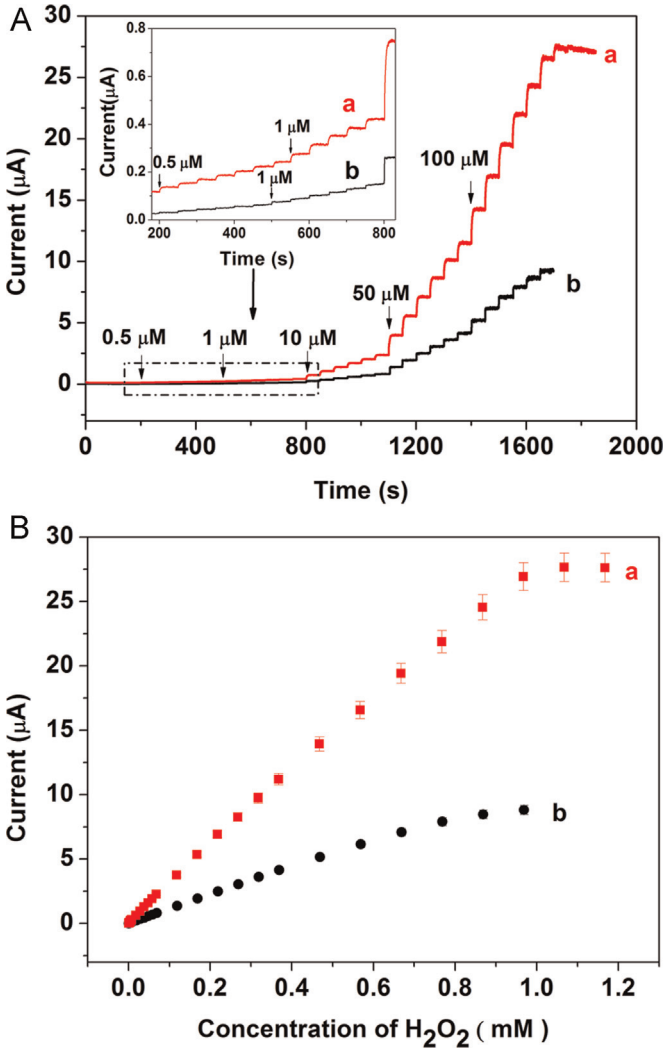

Fig. 4. (A) Amperometric response curves of the HRP/DP–AuNP/GCE (a) and the HRP/GCE (b) at an applied potential of −0.05 V to successive addition of different concentrations of H_2O_2 in N_2-saturated 0.1 M PBS (pH 7.0) containing 1.0 mM HQ. (B) The corresponding calibration curves between the concentration of H_2O_2 and the response current.

shown in Table 1. It could be seen that the HRP/DP–AuNP/GCE showed the highest sensitivity, wider linear range and lowest detection limit relative to those biosensors. The notable enhancement in the performance of the proposed biosensor could be attributed to two reasons. One is the high biocompatibility of the biogenic FF dipeptide utilized (Yan et al., 2007), which is beneficial to preserve enzyme activity. On the other hand, the prepared method for the dipeptide–AuNP hybrid spheres is characteristic relative to the usual AuNPs composites. Most of the AuNPs composites were synthesized using two-step processes involving the preparation of the supported materials, followed by the synthesis and load of AuNPs (Chen et al., 2011; Liu et al., 2012; Wang et al., 2012). Nevertheless, in the present work, the nucleation of gold ion and the self-assembly of FF dipeptide simultaneously happen. The one-step synthesized method is not only simple. More importantly, a large amount of AuNPs could be introduced inside the peptide spheres, at same time localized on the surface of the peptide spheres. The AuNPs localized on the surface of the hybrid spheres can strongly adsorb some proteins and effectively retain their biological activity (Brown et al., 1996; Zhao et al., 1996). Moreover, those AuNPs inside the peptide spheres could act as tiny conduction centers to facilitate electron

Table 1
Comparison of the performances of different H_2O_2 biosensors based on AuNPs composites.

Modified electrode	Sensitivity ($\mu A\ mM^{-1}$)	Linear range (μM)	Detection limit (μM)	Reference
HRP/DP–AuNP/GCE	28.3	0.5–970	0.1	This work
HRP/AuNP–PTA–TNT/[Demim]Br/GCE	10.7	90–1400	6.5	Liu et al. (2013)
HRP/AuNPs–PVA/GCE	–	1–500	0.5	Wang et al. (2012)
HRP/AuNPs/SPAN/GCE	20.27	10–2000	1.6	Chen et al. (2011)
HRP/HIL/GNP–TNT/GCE	16.1	15–750	2.2	Liu et al. (2012)
HRP–GNSs–TiO_2/GCE	–	41–630	5.9	Wang et al. (2010)
HRP/AuNPs–BC/GCE	–	1–500	1.0	Zhang et al. (2010)

PTA, 12-phosphotungstic acid; TNT, TiO_2 nanotube; PVA, poly(vinyl alcohol); SPAN, self-doped polyaniline nanofiber; HIL, hydrophobic ionic liquid; GNP, gold nanoparticle; GNSs, gold nano-seeds; and BC, bacteria cellulose.

transfer between HQ and the bulk electrode surface (Granot et al., 2005; Zhang et al., 2010). Hence, this 3D hybrid structure may lead to a notably enhanced performance for H_2O_2 biosensing including nearly 3-fold increase in the sensitivity and one order of magnitude decrease in the detection limit, in comparison with the control HRP/GCE (curve b in Fig. 4B).

When the concentration of H_2O_2 was higher than 1.0 mM, the catalytic current of the HRP/DP–AuNPs/GCE tended to level off, suggesting a typical Michaelis–Menten process. The apparent Michaelis–Menten constant (K_M^{app}), a reflection of both the enzymatic affinity and the ration of microscopic kinetic constants, was calculated from the electrochemical version of the Lineweave–Burk equation (Gholivand and Khodadadian, 2014). The K_M^{app} value for the HRP/DP–AuNP/GCE was 0.7 mM, which is much smaller than those obtained on some HRP biosensors (Chen et al., 2011; Martin et al., 2014). This result further confirmed that the HRP immobilized on the dipeptide–AuNP hybrid spheres had high bioactivity and great affinity to H_2O_2.

3.6. Selectivity, reproducibility and stability of the biosensor

Interference effects of substances on the HRP/DP–AuNP biosensor were investigated. The potential interfering species, such as glucose, lactate, tyrosine, uric acid and ascorbic acid, were evaluated by comparing the amperometric responses obtained for 0.1 mM H_2O_2 in the absence or presence of each interferent at 0.2 mM concentration. The results were shown in Table S1. Addition of glucose, lactate and tyrosine did not produce observable interference in the biosensor response. However, uric and ascorbic acids may reduce the HQ produced in the HRP catalyzed reaction and thus interfere with the determination of H_2O_2 (Martin et al., 2014).

The reproducibility and stability of the biosensor were also investigated by measuring its current response in 0.1 M PBS containing 1.0 mM HQ and 0.5 mM H_2O_2. The relative standard deviation (R.S.D.) was 3.1% for 7 successive assays using the same enzyme electrode. The reproducibility for five electrodes fabricated in a single batch gave an R.S.D. of 3.3%. In addition, the long-term stability of the biosensor was evaluated after storage at 4 °C for 20 days. The biosensor retained 85.7% of its initial response. These results indicated that the proposed biosensor possessed good stability and acceptable reproducibility.

4. Conclusions

The dipeptide–AuNP hybrid spheres with hollow structure have been successfully fabricated through a simple one-step process. Due to the simultaneous self-assembly of peptides and nucleation of gold ion, the AuNPs were localized both inside and on the surface of the peptide spheres. The unique 3D hybrid spheres have been verified to be a good immobilization matrix for HRP and the prepared mediator biosensor possessed excellent performance, especially displayed higher sensitivity, wider linear range and lower detection limit than some AuNPs composites. The improved performance of the biosensor should be contributed to the excellent biocompatibility of FF dipeptide and the good charge-transport of the hybrid nanostructure. In addition, the biosensor possessed satisfactory reproducibility and long-term stability. Our results show that the self-assembled dipeptide–AuNP hybrid sphere is an attractive electrochemical biosensing platform, and may find wide potential applications in biomedical detection and in-vivo analysis.

Acknowledgments

This work was supported by the National Basic Research Program of China (No. 2011CBA00508), the National Natural Science Foundation of China (No. 21175009) and the Fundamental Research Funds for the Central Universities (YS1406).

Appendix A. Supplementary material

Supplementary data associated with this article can be found in the online version at http://dx.doi.org/10.1016/j.bios.2014.11.029.

References

Adler-Abramovich, L., Badihi-Mossberg, M., Gazit, E., Rishpon, J., 2010. Small 6, 825–831.
Baker, P.A., Goltz, M.N., Schrand, A.M., Yoon, D.Y., Kim, D.S., 2014. Biosens. Bioelectron. 61, 119–123.
Brown, K.R., Fox, A.P., Natan, M.J., 1996. J. Am. Chem. Soc. 118, 1154–1157.
Camacho, C., Chico, B., Cao, R., Matias, J.C., Hernandez, J., Palchetti, I., Simpsond, B.K., Mascinic, M., Villalonga, R., 2009. Biosens. Bioelectron. 24, 2028–2033.
Castillo, J.J., Svendsen, W.E., Rozlosnik, N., Escobar, P., Martineza, F., Castillo-Leon, J., 2013. Analyst 138, 1026–1031.
Chen, C.L., Rosi, N.L., 2010. J. Am. Chem. Soc. 132, 6902–6903.
Chen, X.J., Chen, Z.X., Zhu, J.W., Xu, C.B., Yan, W., Yao, C., 2011. Bioelectrochemistry 82, 87–94.
Chen, X., Cheng, G.J., Dong, S.J., 2001. Analyst 126, 1728–1732.
de La Rica, R., Pejoux, C., Matsui, H., 2011. Adv. Funct. Mater. 21, 1018–1026.
Dickerson, M.B., Sandhage, K.H., Naik, R.R., 2008. Chem. Rev. 108, 4935–4978.
Gazit, E., 2007. Chem. Soc. Rev. 36, 1263–1269.
Gholivand, M.B., Khodadadian, M., 2014. Biosens. Bioelectron. 53, 472–478.
Granot, E., Katz, E., Basnar, B., Willner, I., 2005. Chem. Mater. 17, 4600–4609.
Hamley, I.W., 2014. Angew. Chem. Int. Ed. 53, 6866–6881.
Han, H.S., You, J.-M., Seol, H., Jeong, H., Jeon, S., 2014. Sens. Actuators B: Chem. 194, 460–469.
Kim, J., Sadowsky, M.J., Hur, H.-G., 2011a. Biomacromolecules 12, 2518–2523.
Kim, J.H., Lim, S.Y., Nam, D.H., Ryu, J., Ku, S.H., Park, C.B., 2011b. Biosens. Bioelectron. 26, 1860–1865.
Knowles, T.P.J., Oppenheim, T.W., Buell, A.K., Chirgadze, D.Y., Welland, M.E., 2010. Nat. Nanotechnol. 5, 204–207.
Liu, X.Q., Feng, H.Q., Zhang, J.M., Zhao, R.X., Liu, X.H., Wong, D.K.Y., 2012. Biosens. Bioelectron. 32, 188–194.
Liu, X.Q., Zhang, J.M., Liu, S.H., Zhang, Q.Y., Liu, X.H., Wong, D.K.Y., 2013. Anal. Chem. 85, 4350–4356.

Martin, M., Salazar, P., Villalonga, R., Campuzano, S., Pingarrón, J.M., González-Mora, J.L., 2014. J. Mater. Chem. B 2, 739–746.
Nayak, N.C., Shin, K., 2006. J. Nanosci. Nanotechnol. 6, 3512–3516.
Panda, J.J., Mishra, A., Basu, A., Chauhan, V.S., 2008. Biomacromolecules 9, 2244–2250.
Park, B.W., Zheng, R., Ko, K.A., Cameron, B.D., Yoon, D.Y., Kim, D.S., 2012. Biosens. Bioelectron. 38, 295–301.
Qu, F.L., Zhang, Y., Rasooly, A., Yang, M.H., 2014. Anal. Chem. 86, 973–976.
Reches, M., Gazit, E., 2004. Nano Lett. 4, 581–585.
Reches, M., Gazit, E., 2006. Curr. Nanosci. 2, 105–111.
Ryu, J., Lim, S.Y., Park, C.B., 2009. Adv. Mater. 21, 1577–1581.
Sasso, L., Vedarethinam, I., Emnéus, J., Svendsen, W.E., Castillo-León, J., 2012. J. Nanosci. Nanotechnol. 12, 3077–3083.
Silvestrini, M., Fruk, L., Ugo, P., 2013. Biosens. Bioelectron. 40, 265–270.
Singh, S., Topuz, F., Hahn, K., Albrecht, K., Groll, J., 2013. Angew. Chem. Int. Ed. 52, 3000–3003.
Song, C.Y., Zhao, G.P., Zhang, P.J., Rosi, N.L., 2010. J. Am. Chem. Soc. 132, 14033–14035.
Tan, Y.N., Lee, J.Y., Wang, D.I.C., 2010. J. Am. Chem. Soc. 132, 5677–5686.
Ulijn, R.V., Smith, A.M., 2008. Chem. Soc. Rev. 37, 664–675.
Wang, J., Yao, H.B., He, D.A., Zhang, C.L., Yu, S.H., 2012. ACS Appl. Mater. Int. 4, 1963–1971.
Wang, G.H., Zhang, L.M., 2006. J. Phys. Chem. 110, 24864–24868.
Wang, Y., Ma, X.L., Wen, Y., Xing, Y.Y., Zhang, Z.R., Yang, H.F., 2010. Biosens. Bioelectron. 25, 2442–2446.
Whitesides, G.M., Grzybowski, B., 2002. Science 295, 2418–2421.
Won, Y.H., Aboagye, D., Jang, H.S., Jitianu, A., Stanciu, L.A., 2010. J. Mater. Chem. 20, 5030–5034.
Xiao, Y., Ju, H.X., Chen, H.Y., 1999. Anal. Chim. Acta 391, 73–82.
Yan, X.H., He, Q., Wang, K.W., Duan, L., Cui, Y., Li, J.B., 2007. Angew. Chem. Int. Ed. 46, 2431–2434.
Yan, X.H., Zhu, P.L., Fei, J.B., Li, J.B., 2010a. Adv. Mater. 22, 1283–1287.
Yan, X.H., Zhu, P.L., Li, J.B., 2010b. Chem. Soc. Rev. 39, 1877–1890.
Yemini, M., Reches, M., Gazit, E., Rishpon, J., 2005a. Anal. Chem. 77, 5155–5159.
Yemini, M., Reches, M., Rishpon, J., Gazit, E., 2005b. Nano Lett. 5, 183–186.
Yin, H.S., Zhang, Q.M., Zhou, Y.L., Ma, Q., Liu, T., Zhu, L.S., Ai, S.Y., 2011. Electrochim. Acta 56, 2748–2753.
Zhang, T.J., Wang, W., Zhang, D.Y., Zhang, X.X., Ma, Y.R., Zhou, Y.L., Qi, L.M., 2010. Adv. Funct. Mater. 20, 1152–1160.
Zhao, J., O'Daly, J.P., Henkens, R.W., Stonehuerner, J., Crumbliss, A.L., 1996. Biosens. Bioelectron. 11, 493–502.